Geosci. Instrum. Method. Data Syst. Discuss., 5, 577–598, 2015
www.geosci-instrum-method-data-syst-discuss.net/5/577/2015/
doi:10.5194/gid-5-577-2015

Geoscientific Instrumentation Methods and Data Systems Discussions
Open Access

Weather model verification using Sodankylä mast measurements

M. Kangas, L. Rontu, C. Fortelius, M. Aurela, and A. Poikonen

Finnish Meteorological Institute, Meteorological Research, P.O. Box 503, 00101 Helsinki, Finland

Received: 4 December 2015 – Accepted: 10 December 2015 – Published: 21 December 2015

Correspondence to: M. Kangas (markku.kangas@fmi.fi)

Published by Copernicus Publications on behalf of the European Geosciences Union.

Abstract

Sodankylä, in the heart of Arctic Research Centre of the Finnish Meteorological Institute (FMI ARC) in northern Finland, is an ideal site for atmospheric and environmental research in the boreal and sub-arctic zone. With temperatures ranging from −50 to +30 °C, it provides a challenging testing ground for numerical weather forecasting (NWP) models as well as weather forecasting in general. An extensive set of measurements has been carried out in Sodankylä for more than 100 years. In 2000, a 48 m high micrometeorological mast was erected in the area. In this article, the use of Sodankylä mast measurements in NWP model verification is described. Started in 2000 with NWP model HIRLAM and Sodankylä measurements, the verification system has now been expanded to include comparisons between 12 NWP models and seven measurement masts. A case study, comparing forecasted and observed radiation fluxes, is also presented. It was found that three different radiation schemes, applicable in NWP model HARMONIE-AROME, produced during cloudy days somewhat different downwelling long-wave radiation fluxes, which however did not change the overall cold bias of the predicted screen-level temperature.

1 Introduction

Nocturnal and winter-time surface temperature inversions still pose a difficult challenge to weather forecast models. For the model development, versatile measurements are essential. The Arctic Research Centre of the Finnish Meteorological Institute (FMI ARC, http://fmiarc.fmi.fi/), is well suited for this purpose. The FMI ARC consists of two main stations, the headquarters in Sodankylä (67.368° N, 26.633° E), and the Pallas clean air research station (67.967° N, 24.117° E), which both provide ideal location for atmospheric and environmental research in the boreal and sub-arctic zone.

FMI-ARC dates back to the mid-nineteenth century when, in 1858, The Societas Scientarum Fennica founded the first weather station in Sodankylä. Continuous meteorological measurements were started in 1908 and have been continued to this day (Savunen et al., 2014). Being accessible from all parts of the world, FMI ARC is also an excellent base for studying various themes of global change in a northern context.

Today, an extensive set of measurements ranging from basic meteorological data to heat and carbon fluxes as well as ozone and arctic snow coverage measurements is being performed at FMI ARC. Sodankylä observatory provides also facilities for receiving and processing polar satellite images, and FMI has conducted systematic aurora observations in the Finnish Lapland since late 1950's. The FMI ARC research sites belong to the Lapland Biosphere–Atmosphere Facility (LAP-BIAT, http://www.sgo.fi/lapbiat/), an infrastructure project through which the EU can fund visiting research groups. It has also been a site for various measurement campaigns (e.g., NOPEX/WINTEX campaign in 1997, Halldin et al., 2001), as well as various EU projects and measurement networks (e.g. CEOP, CarboEuropeIP, ICOS).

In the weather model verification, the traditional way is to perform detailed studies of model analyses and forecasts by comparing them with measurements afterwards. Another way to provide insight into model behaviour is to compare measurements with forecasts parallel with model runs in near-real time. Although based partly on less accurate (unchecked) measurements, this approach nevertheless provides valuable information about model behaviour and, when monitored frequently, can also act as a kind of alarm bell, alerting model developers when there are apparent problems with model forecasts. As added benefit, it provides means to monitor measurements.

Starting from 2000, the measurements at FMI ARC have been used to verify weather model forecasts in near-real time. The verification was started with NWP model HIRLAM (Undén et al., 2002; Eerola, 2013) and Sodankylä measurements, but has later been extended to cover several other NWP models and mast measurement stations. Presently, a total of 12 models and seven measurement masts are included. The models represent the activities of HIRLAM (http://hirlam.org) and ALADIN (http://www.cnrm.meteo.fr/aladin/) NWP consortia, as well as those of ECMWF (European Centre for Medium-Range Weather Forecast, http://www.ecmwf.int/). The

GID
5, 577–598, 2015

forecast-measurement comparison plots with statistical analyses are provided on-line as a part of HIRLAM forecast runs.

The harmonized and quality checked datasets collected in Sodankylä are also available for more detailed research and model development. From the point of view of research, the most valuable feature of the Sodankylä site is that it offers the possibility to combine various simultaneous measurements, including those from a micrometeorological mast and a radiation tower, as well as from dedicated snow and soil observations, AWS and atmospheric soundings. In this article, these datasets are utilized in a study of radiation from HARMONIE-AROME forecast system (Seity et al., 2011) vs. measured radiation in Sodankylä.

Section 2 contains description of Sodankylä site and Sect. 3 of the mast verification system. A comparative study on HARMONIE-AROME radiation schemes is presented in Sect. 4, and conclusions in Sect. 5.

2 Sodankylä measurements

The terrain around FMI ARC Sodankylä observatory (67.368° N, 26.633° E, altitude 179 m a.s.l., http://fmiarc.fmi.fi/) is moderately undulating, with isolated fells reaching up to 500 m altitude. The observatory is located on the eastern bank of the river Kitinen, seven kilometres southeast of the Sodankylä town centre, and about 100 km north of the Polar Circle and Rovaniemi. The vegetation in Sodankylä area is typical for the northern boreal zone, with coniferous forest (mostly managed) and large open mires dominating the landscape. The climate is characterised by long and cold continental-type winters and relatively warm but short summers. During 1981–2010, the average yearly medium screen level temperature was −0.4 °C, yearly precipitation 527 mm, and snow cover duration 200 days (from 26 October to 14 May). The absolute minimum screen level temperature during the same period was −49.5 °C and with absolute maximum at +30.0 °C.

GID
5, 577–598, 2015

Due to the warming effect of the Gulf Stream the area can be classified as continental subarctic or boreal taiga, by Köppen classification climate region Dfc (continental subarctic or boreal (taiga) climates). However, with regard to stratospheric meteorology, Sodankylä can be classified as an arctic site, often lying beneath the middle or the edge of the stratospheric polar vortex and in a zone displaying intermittent polar stratospheric ozone depletion (Savunen et al., 2014).

Continuous meteorological measurements have been performed in Sodankylä since 1908. Ground-station observations every three hours record information on weather conditions prevailing at ground level. In addition to standard weather observations, the basic observational duties at the Observatory include regular recordings of solar radiation, sunshine and hydrological quantities. Radiosonde measurements are carried out twice a day. In 2000, a micrometeorological mast (48 m) for atmospheric boundary layer measurements was erected in the area and has since been producing data.

Sodankylä has also been extensively utilized for measurements in various projects, e.g. NOPEX and WINTEX in 1997 (Halldin et al., 2001), and CEOP (Savunen et al. (2014), http://data.eol.ucar.edu/master_list/?project=CEOP/EOP-3/4). During NOPEX/WINTEX an additional mast (18 m) was temporarily erected and used (Batchvarova et al., 2001). An aircraft campaign to measure boundary layer properties was also performed during NOPEX/WINTEX (Kangas et al., 2001).

Data from most of the measurements is collected into a central data base at http://litdb.fmi.fi/. It contains data not only from Sodankylä but also from other FMI ARC measurement sites. In the following, the measurements used in the mast verification are briefly described.

2.1 Micrometeorological mast

In 2000, a 48 m high micrometeorological mast was erected in the immediate vicinity of the Sodankylä observatory (http://litdb.fmi.fi/micrometeorologicalmast.php). The height of the mast was limited by the presence of a near-by airfield. It is located in a sparse Scots pine forest on a sandy podzol. The average tree height in is 12 m, tree density

210 000 trunks km^{-2}, tree age 60–160 years, and the projected leaf area 1.2 m^2 (http://en.ilmatieteenlaitos.fi/GHG-measurement-sites).

The mast is extensively instrumented with temperature, wind, humidity, and radiation measurements at various levels (Fig. 1, Table 2). The instruments used include PT100 (Pentronic) thermometers for temperature, HMP35/45D (Vaisala) humidity sensors, and WAAA25 (Vaisala) anemometers. Downwelling and upwelling short wave and long wave radiation components (CNR4, Kipp&Zonen), net radiation (Nr-Lite, Kipp&Zonen) and photosynthetically active radiation (PAR, LI190Z, Licor) are measured at the top of the tower (48 m). Heat and momentum fluxes are measured at the 23 m level by the eddy covariance method (see more detailed description below).

Additional near-ground measurements including soil temperature and soil moisture profiles, soil heat flux, snow depth, and below canopy PAR are performed in the vicinity of the mast (http://litdb.fmi.fi/micrometeorologicalmastfield.php).

2.2 Heat and momentum fluxes

The in situ fluxes of sensible heat, latent heat and momentum are measured at the micrometeorological mast by the micrometeorological eddy covariance (EC) method, which provides direct measurements of the fluxes averaged on an ecosystem scale. In the EC method, the vertical flux is obtained as the covariance of the high frequency (10 Hz) observations of vertical wind speed and the variable in question (temperature, H_2O concentration or horizontal wind speed) (Baldocchi, 2003).

The eddy covariance measurement system at Sodankylä includes a USA-1 (METEK GmbH, Elmshorn, Germany) three-axis sonic anemometer/thermometer and a closed-path LI-7000 (Li-Cor., Inc., Lincoln, NE, USA) CO_2/H_2O gas analyser. The measurements are performed at 23 m, 5 to 10 m above the mean forest height. The EC fluxes are calculated as half-hourly averages taking into account the appropriate corrections. The measurement systems and the post-processing procedures are presented in more detail by and Thum et al. (2009) and Aurela et al. (2015). See also Table 2.

GID
5, 577–598, 2015

2.3 Solar radiation tower

In addition to the basic synoptic measurements, a set of additional measurements is performed on a 18 m high solar radiation tower in the observatory area. It contains measurements of main radiation components: short wave radiation (CM11, Kipp&Zonen), direct normal radiance (NIP, Eppley), long wave radiation (CG4 Kipp&Zonen) and aerosol optical depth (PFR-N32, PMOD/WRC) (http://litdb.fmi.fi/radiationtower.php).

For consistency, all radiation data used in the mast verification is obtained from the radiation tower. The measurements instruments on the radiation tower are also easily reachable and allow more frequent maintenance than those on the micrometeorological mast.

2.4 Automatic weather station

The automatic weather station (AWS) providing the official main weather parameters from Sodankylä. AWS has been in use since February 2008. All the instruments and sensors at the station are calibrated annually. The parameters include screen level temperature (PT100, Pentronic) and humidity (HMP, Vaisala), air pressure (PTB201A, Vaisala), visibility (FD12P, Vaisala), and cloudiness (CT25K, Vaisala). Wind speed and gust (WAA25, Vaisala) and wind direction (WAV15, Vaisala) at the height of 22 m, as well as snow depth (SR50, Campbell Scientific) are also provided (http://litdb.fmi.fi/apache2-default/luo0015_data.php).

3 The mast verification system

3.1 Near-real-time comparison

Since 2000, near-real-time comparisons of model forecasts and in situ measurements have been performed as a part of HIRLAM weather forecast model operational runs at FMI. Started with HIRLAM forecast and Sodankylä measurements, the comparison

GID
5, 577–598, 2015

has expanded to comprise a total of 12 models and seven masts from around Europe. An eighth mast in Estonia is presently being introduced into the system (Table 1). In addition to the direct on-line comparison, long-term comparison statistics are provided.

To enable rapid update of the comparison, the comparison plots are produced as a part of the operational HIRLAM forecast cycle (currently four times a day after synoptic hours 00:00, 06:00, 12:00, and 18:00 UTC) using the latest available data.

The HIRLAM program web site (http://hirlam.org) is used as the data pool, into which the data providers transfer their data in prescribed format and from where it is retrieved by the plotting routines located at FMI. The plotting is performed with Gnuplot (http://www.gnuplot.info/) scripts, produced and run by the data retrieving program based on perl and unix scripts.

The parameters that are currently plotted include temperature, wind speed, and humidity at specified levels as well as various heat and radiation fluxes (Table 2). With the original aim in mind, the temperature difference between two metres and at a higher level (usually the first model level) is also included in the plots as a measure of the surface temperature inversion. For all masts and models, the full set of parameters is not available, in which case an appropriate subset is plotted. A sample plot showing 2 m temperature from HIRLAM forecast as compared to Sodankylä measurements is shown in Fig. 2.

The interactive web page that has been set up for browsing the comparison results is visualised in Fig. 3. There are two panes, on each of which the user can select the desired mast/model combination. By scrolling down the page, comparison for different parameters can be viewed.

Not all model-mast-parameter combinations are possible, however, because parameters measured at different masts vary and all mast locations are not covered by all model integration areas. In these cases, a special "No comparison available" plot is shown. The web page also contains information about the parameters as well as brief descriptions of the masts and models included in the comparison. The page is available to all HIRLAM and ALADIN consortia participants and to data suppliers as a part of the general HIRLAM forecast visualisation pages.

3.2 Statistical comparison

Seasonal statistics compiled for individual observatories, or mast sites, containing the models available at each respective station are also calculated in the mast comparison. Seasonal summaries of the daily comparisons, including a variety of descriptive and comparative statistics, are shown under a separate heading on the interactive web page.

Graphs include time series of observed and modelled variables and the departures of model output from the observations. They provide a qualitative view of how the models are doing, and how their performance has varied during the season, thus linking model performance to the prevailing conditions. These graphs are also useful for identifying gaps in the data.

Graphs of average model biases and rms-errors as function of forecast lead time serve to quantify the errors, while scatterplots, histograms and mean diurnal cycles help to interpret the errors physically by linking the average errors to specific conditions or hours of the day.

4 Comparison of HARMONIE-AROME radiation fluxes to Sodankylä observations: a case study

Spectrally averaged shortwave and longwave radiation fluxes at the surface are predicted output variables of the contemporary NWP models. They are directly comparable to the observed radiation fluxes, which could thus be used for the validation of the forecast along with the near-surface temperature and humidity, anemometer-level wind, cloudiness and other variables diagnosed from the NWP model output in the standard station verification. In particular, comparison of the simulated and ob-

GID
5, 577–598, 2015

served radiation fluxes can give useful insight for the development of the cloud and radiation parametrizations in the NWP models. Both in reality and in the models, the short-term variability of the surface radiation fluxes is mostly related to the variations of cloud and aerosol particles in air. In Sodankylä, the influence of aerosol in the atmospheric radiation transfer is minor. In this section, we will test different atmospheric radiation parametrizations in an experimental version of the HARMONIE-AROME forecast system, based on cycle 38h1.2 (http://hirlam.org/index.php/hirlam-programme-53/general-model-description/mesoscale-harmonie), against the Sodankylä radiation tower measurements.

4.1 Measurements and numerical experiments

For a model-observation comparison, six components of radiation fluxes measured in the 18 m high Sodankylä radiation tower are available (Table 2): shortwave downwards (SWD or global radiation) and upwards (reflected), direct normal solar irradiance (DNI), diffuse short wave solar radiation, long wave radiation downwards (LWD) and upwards. In this study, we compared the observed SWD and LWD to their model counterparts for time period 15 January–15 May 2014. The available one-minute flux measurements were averaged over three-hour periods and compared with the three-hour average fluxes derived from the accumulated radiation fluxes of the +6 and +3 h HARMONIE-AROME forecasts, which were initiated every 6 h (00:00, 06:00, 12:00, 18:00 UTC). In addition, the screen-level temperature observations provided by the Sodankylä automatic weather station (AWS), representing the middle of each three-hour period, were selected for comparison with the forecasted screen-level temperature. Sodankylä daily average precipitation observations were extracted from FMI climatological data base.

The default atmospheric radiation parametrization of AROME (Seity et al., 2011) is based on the radiation transfer code in the Integrated Forecast System (IFS cycle 25R1, European Centre for Medium-Range Weather Forecast implementation in 2002; see ECMWF, 2012; Mascart and Bougeault, 2011), denoted here as IFSRAD. An alternative radiation scheme originates in ALADIN (Mašek et al., 2015), hereafter denoted

GID
5, 577–598, 2015

as ACRANEB2. The radiation scheme of HIRLAM, based on Savijärvi (1990) (see also Nielsen et al., 2014), hereafter denoted as HLRADIA, is available for experimentation. All three schemes were tested within the framework of AROME physical parametrizations by running three series of HARMONIE-AROME experiments over a domain covering Finland. A horizontal resolution of 2.5 km and 65 levels in vertical were used. Lateral boundary conditions for the experiments were obtained from the ECMWF analyses. For the initial state of each +27 h forecast, the objective analysis of the surface variables was combined with the atmospheric analysis extracted from the boundary files.

4.2 Model–observation comparison in spring 2014

Most of the days during 15 January–15 March 2014 were cloudy in Sodankylä. Most observed and predicted clouds were essentially non-precipitating. The non-precipitating clouds predicted by HARMONIE-AROME consisted mainly of (super-cooled) liquid droplets while the ice crystal content was small. Some amount of (precipitating) snow and graupel was practically always present in the simulated clouds. This is due to a recent change in cloud microphysics treatment in the reference system (Karl-Ivar Ivarsson, personal communication, 2015). A small amount of liquid/ice condensate at the lowest model level was often predicted.

Every month, there were several days when more than one mm of precipitation, corresponding roughly to one cm of snowfall, was observed and predicted, while the first significant rainfall appeared in the end of April. These precipitation events were predicted well by the model. Falling precipitation was observed during the periods when also HARMONIE suggested significant snow and graupel content in the clouds. This indicates that in the model, most particles classified as precipitating indeed reached the surface, in agreement with the observations. Typically, the simulated condensate content of the precipitating particles was two to three times the liquid droplet water content, which in turn was an order of magnitude larger than that of the ice water content. In our experiments, only the cloud liquid droplets and ice crystals, but not the precipi-

GID
5, 577–598, 2015

tating particles, were allowed to influence the radiative transfer in the atmosphere. This deviated from the reference system where a fraction of the snow and graupel particles is accounted for when determining the cloud optical properties.

Figure 4 shows time-series of the observed and forecasted (+24 h) screen-level temperature, SWD and LWD as well as the difference between the observed and forecasedt LWD in February 2014. An overall cold bias of the screen-level temperature forecast by the model using any radiation scheme was detected as compared to the AWS observations (Fig. 4a). Typically, forecast was one-two degrees colder than observed.

In February, solar radiation flux (Fig. 4b) is small, Sodankylä being located north from the polar circle. In February 2014, the maximum observed SWD value was ca 160 W m^{-2}, while a typical daily maximum value was less than 80 W m^{-2}. As the long-wave effects (Fig. 4c) are expected to dominate in the surface radiation balance, we will focus to the LWD comparison.

Generally, the LWD flux was predicted well (Fig. 4c and d). The largest differences between predicted and observed LWD were found 1–2, 7–8 and 19–21 February. The results were best when using the IFSRAD and ACRANEB2 schemes, while more deviations were found for HLRADIA.

Automatic weather station observations (not shown) indicated that during February 2014, only the afternoon and night after the 20th was cloudless in Sodankylä. In this truly clear sky case (both observed and simulated) all schemes correctly produced small LWD fluxes and low screen-level temperatures. When observed clouds were not caught by the model, LWD fluxes were underestimated by all schemes. This was the case e.g. on 21 February. Downwelling long-wave radiation was overestimated by HLRADIA (Fig. 4c and d) when the simulated clouds were optically thick (due to the assumed large super-cooled liquid water content, not shown), for example during 9–12 February. During some periods (7–8 and 17–19 February), the cold bias of the screen-level temperature was most evident for HLRADIA, which showed the most underestimated LWD values these days. Also the integrated cloud liquid water content

GID
5, 577–598, 2015

was then smaller in the experiment with HLRADIA than it was with other schemes. This might indicate secondary effects due to the cloud-radiation interactions in the model. However, more studies are needed to estimate the significance of this difference and to understand the mechanism behind it.

The different LWD produced by the different radiation schemes does not, however, explain the systematic bias of the predicted screen-level temperature. LWD is a part of the surface energy balance, which determines the (snow, soil) surface temperature that interacts with the atmosphere. In the model, the diagnostic screen-level temperature is obtained by interpolating between the predicted lowest model level (representing the layer up to ca 28 m from the surface) and the surface temperatures. In the interpolation, the surface layer stability is taken into account.

The simulated upwelling long-wave radiation (not shown), which represents the surface temperature, followed observations generally much more closely than the screen-level temperature. This indicates that the surface (skin) temperature seen by the radiation parametrizations was predicted well in most cases (with the exception of the first two days and 7–8 February). Thus, the simulated screen-level temperature was evidently strongly influenced by the lowest model level temperature, which in turn was dominated by the temperature advection in the low troposphere. In a model-observation comparison at a single location, phase errors of the large-scale forecast in time and space show up if e.g. the arrival of an atmospheric frontal system has been forecasted incorrectly. However, a systematic bias is hardly explained by the phase errors. A comparison between the predicted lowest model level temperature with the corresponding measurements of the micrometeorological mast, as well as a comparison between the predicted surface temperature and the corresponding snow/soil surface temperatures, might shed light to the problem. Predicted solar radiation fluxes, although small in this period, deserve evaluation against the observations. This falls, however, outside the scope of the present study.

GID
5, 577–598, 2015

5 Conclusions

The near-real time mast verification of NWP forecasts, started in 2000, has proved to be very useful in NWP model verification and, after being started with only one model and one mast (HIRLAM and Sodankylä), has now expanded to include 12 forecasts and seven masts.

The mast verification system has been integrated with the operative runs of NWP model HIRLAM, with data for other models and masts obtained through a common data pool. The results are shown as a part of HIRLAM web-based visualisation pages that are available to all data suppliers and members of HIRLAM and ALADIN NWP model consortia. The system is not dependent on HIRLAM runs, though, and could be also run separately.

Statistics of the comparisons with e.g. long-term bias are also included in the verification, although they are not updated daily but on seasonal basis. They provide seasonal summaries of the daily comparisons, including a variety of descriptive and comparative statistics.

A comparative study of different radiation schemes applicable within HARMONIE-AROME NWP system was also presented for spring 2014. Based on this example, we conclude that the three different radiation schemes produced generally good but somewhat different LWD fluxes in cloudy days – and in February 2014, there was only one afternoon and night free of clouds in Sodankylä. The HLRADIA scheme behaved most differently from the other two schemes – IFSRADIA and ACRANEB2. HLRADIA tended to overestimate LWD in case of optically thick clouds and possibly underestimate it in case of optically thin clouds. However, when comparing the simulated screen-level temperatures to those observed by AWS, the usage of any scheme seemed to lead to a systematic cold bias of the order of one to two degrees. The reason of this bias seems to lay outside the radiation parametrizations and requires further study to be understood.

GID
5, 577–598, 2015

Acknowledgements. The co-operation of Riika Ylitalo and Ari Aaltonen from the Finnish Meteorological Institute is gratefully acknowledged. The co-operation and interest of the Hirlam and Aladin consortia and the efforts of the data providers have been essential in the setting up of the on-line verification system.

References

Aurela, M., Lohila, A., Tuovinen, J.-P., Hatakka, J., Penttilä, T., and Laurila, T.: Carbon dioxide and energy flux measurements on four different northern boreal ecosystems at Pallas, Boreal Environ. Res., 20, 455–473, 2015.

Baldocchi, D.: Assessing the eddy covariance technique for evaluating carbon dioxide exchange rates of ecosystems: past, present and future, Global Change Biol., 9, 479–492, 2003.

Batchvarova, E., Gryning, S.-E., and Bay Hasager, C.: Regional fluxes of momentum and sensible heat over a sub-arctic landscape during late winter, Bound.-Lay. Meteorol., 99, 489–507, 2001.

ECMWF: IFS Documentation cy38r1, Part IV: Physical Processes, available at: https://software.ecmwf.int/wiki/display/IFS/CY38R1+Official+IFS+Documentation (last access: December 2015), 2012.

Eerola, K.: Twenty-one years of verification from the HIRLAM NWP system, Weather Forecast., 28, 270–285, 2013.

Halldin, S., Gryning, S.-E., and Lloyd, C. R. (guest editors): Land-surface/atmosphere exchange in high-latitude landscapes, Theor. Appl. Climatol., 70, 1–252, doi:10.1007/s007040170001, 2001.

Kangas, M., Heikinheimo, M., and Laine, V.: Accuracy of NOAA AVHRR-based surface reflectances over winter-time boreal surface – comparison with aircraft measurements and land-cover information, Theor. Appl. Climatol., 70, 231–244, 2001.

Mascart, P. J. and Bougeault, P.: The Meso-NH Atmospheric Simulation System: Scientific Documentation, Tech. rep., Meteo France, Toulouse, France, 2011.

Mašek J., Geleyn, J. F., Brožková R., Giot, O., Achom, H. O., and Kuma, P.: Single interval shortwave radiation scheme with parameterized optical saturation and spectral overlaps, Q. J. Roy. Meteorol. Soc., doi:10.1002/qj.2653, in press, 2015.

Nielsen, K. P., Gleeson, E., and Rontu, L.: Radiation sensitivity tests of the HARMONIE 37h1 NWP model, Geosci. Model Dev., 7, 1433–1449, doi:10.5194/gmd-7-1433-2014, 2014.
Savijärvi, H.: Fast radiation parameterization schemes for mesoscale and short-range forecast models, J. Appl. Meteorol., 29, 437–447, 1990.
Seity, Y., Brousseau, P., Malardel, S., Hello, G., Benard, P., Bouttier, F., Lac, C., and Masson, V.: The AROME-France convective-scale operational model, Mon. Weather Rev., 139, 976–991, 2011.
Savunen, T., Kivi, R., Poikonen, A., Kangas, M., Säntti, K., Hyvönen, R., Mammarella, I., Gregow, E., and Tammelin, B.: CEOP Reference site – Sodankylä, Finland, Finnish Meteorological Institute, Reports 2014:9, available at https://helda.helsinki.fi/bitstream/handle/10138/157360/2014nro9.pdf?sequence=3 (last access: December 2015), 2014.
Thum, T., Aalto, T., Laurila, T., Aurela, M., Hatakka, J., Lindroth, A., and Vesala, T.: Spring initiation and autumn cessation of boreal coniferous forest CO_2 exchange assessed by meteorological and biological variables, Tellus B, 61, 701–717, 2009.
Undén, P., Rontu, L., Järvinen, H., Lynch, P., Calvo, J., Cats, G., Cuxart, J., Eerola, K., Fortelius, C., Garcia-Moya, J. A., Jones, C., Lenderlink, G., McDonald, A., McGrath, R., Navascues, B., Woetman Nielsen, N., Odegaard, V., Rodriguez, E., Rummukainen, M., Room, R., Sattler, K., Hansen Sass, B., Savijärvi, H., Wichers Schreur, B., Sigg, R., The, H., and Tijm, A.: HIRLAM-5 scientific Documentation, HIRLAM-5, available at: http://hirlam.org/ (last access: December 2015), 2002.

GID
5, 577–598, 2015

Weather model verification using Sodankylä mast measurements

M. Kangas et al.

Table 1. Masts and weather forecast models included in the mast verification.

Mast	Model
Sodankylä (Finland)	HIRLAM RCR (FMI)
Cabauw (the Netherlands)	HIRLAM Spain (AEMet, Spain)
Valladolid (Spain)	ARPEGE (Météo-France)
Lindenberg (Germany)	ALADIN (Météo-France)
Valgjärve (Estonia) [1]	AROME (Météo-France)
Kivenlahti (Finland)	"Mini-AROME" (Météo-France)
Kuopio (Finland)	HARMONIE-AROME (FMI)
Rovaniemi (Finland)	IFS (ECMWF)
	IFS disseminated to FMI [2]
	LAPS analysis system (FMI)
	LAPS Scandinavian area (FMI)
	Meteorologist's editor (FMI) [3]

[1] Upcoming.
[2] IFS data as disseminated to FMI, partly interpolated.
[3] Forecast data edited by duty meteorologists.

GID
5, 577–598, 2015

GID
5, 577–598, 2015

Weather model verification using Sodankylä mast measurements

M. Kangas et al.

Title Page
Abstract Introduction
Conclusions References
Tables Figures
◂ ▸
Back Close
Full Screen / Esc
Printer-friendly Version
Interactive Discussion

Table 2. Comparison parameters (parameters 1–5 and 12–15 are from the micrometeorological mast, 6–11 from the radiation tower).

Parameter	Unit	Instrument ǀ Manufacturer
1. Air temperature, level 1 (2 m)	°C	PT100 ǀ Pentronic AB
2. Air temperature, level 2*	°C	PT100 ǀ Pentronic AB
3. Temperature difference betw. levels 1 and 2	°C	[calculated]
4. Relative humidity	%	HMP35/45D ǀ Vaisala Oyj
5. Wind speed (10 m)	$\mathrm{m\,s^{-1}}$	WAA25 ǀ Vaisala Oyj
6. Short wave solar radiation, incoming	$\mathrm{W\,m^{-2}}$	CM11 ǀ Kipp & Zonen
7. Short wave solar radiation, outgoing (refl.)	$\mathrm{W\,m^{-2}}$	CM11 ǀ Kipp & Zonen
8. Direct normal short wave solar radiation	$\mathrm{W\,m^{-2}}$	NIP ǀ Eppley
9. Diffuse short wave solar radiation	$\mathrm{W\,m^{-2}}$	CM11 ǀ Kipp & Zonen
10. Long wave radiation, incoming	$\mathrm{W\,m^{-2}}$	CG4 ǀ Kipp & Zonen
11. Long wave radiation, outgoing	$\mathrm{W\,m^{-2}}$	CG4 ǀ Kipp & Zonen
12. Momentum flux	$\mathrm{N\,m^{-2}}$	LI-7000/USA-1 ǀ Licor/METEK
13. Sensible heat flux	$\mathrm{W\,m^{-2}}$	LI-7000/USA-1 ǀ Licor/METEK
14. Latent heat flux	$\mathrm{W\,m^{-2}}$	LI-7000/USA-1 ǀ Licor/METEK
15. Evaporation	$\mathrm{mm\,h^{-1}}$	LI-7000/USA-1 ǀ Licor/METEK

* Usually the lowest model level.

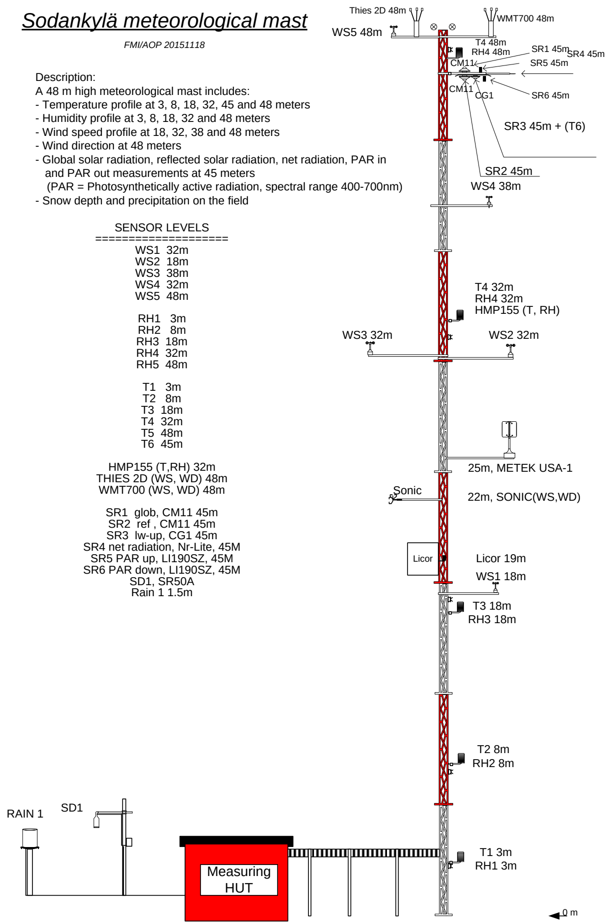

Figure 1. Sodankylä micrometeorological mast (November 2015). WS = wind speed, RH = relative humidity, T = temperature, SR = solar radiation, SD = snow depth (Poikonen, 2015).

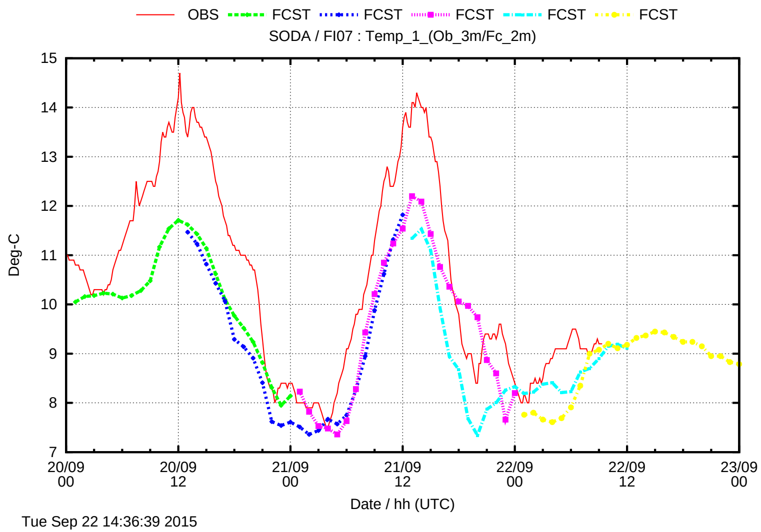

Figure 2. Example mast verification plot: 2 m temperature from HIRLAM forecast compared to Sodankylä measurements. Red continuous line (OBS) shows measurements, dotted coloured lines (FCST) show the first 24 h from a set of consecutive forecasts.

GID
5, 577–598, 2015

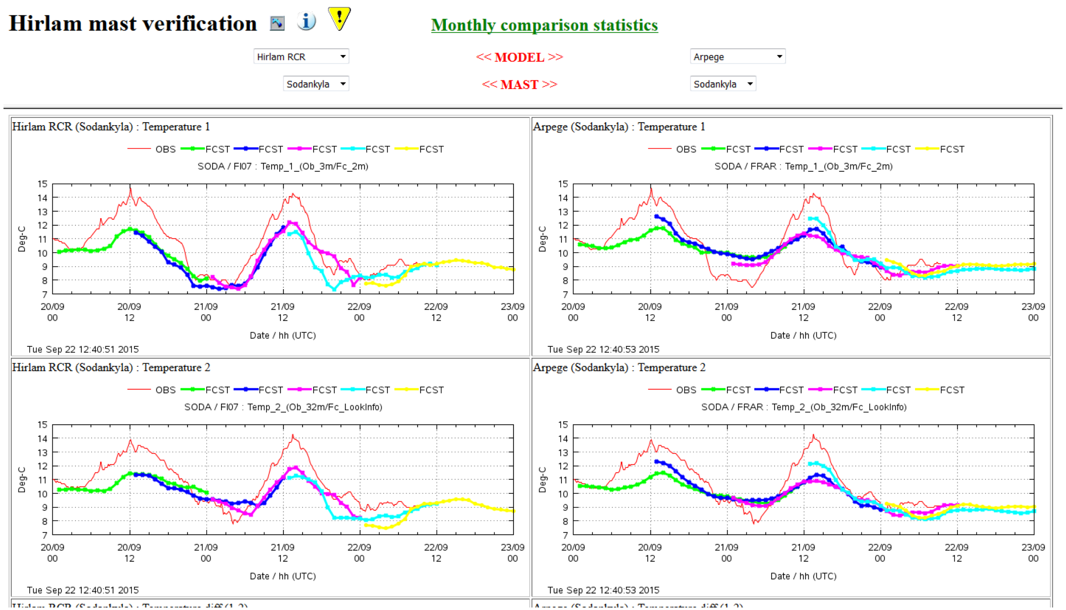

Figure 3. Web page sample.

GID
5, 577–598, 2015

Weather model verification using Sodankylä mast measurements

M. Kangas et al.

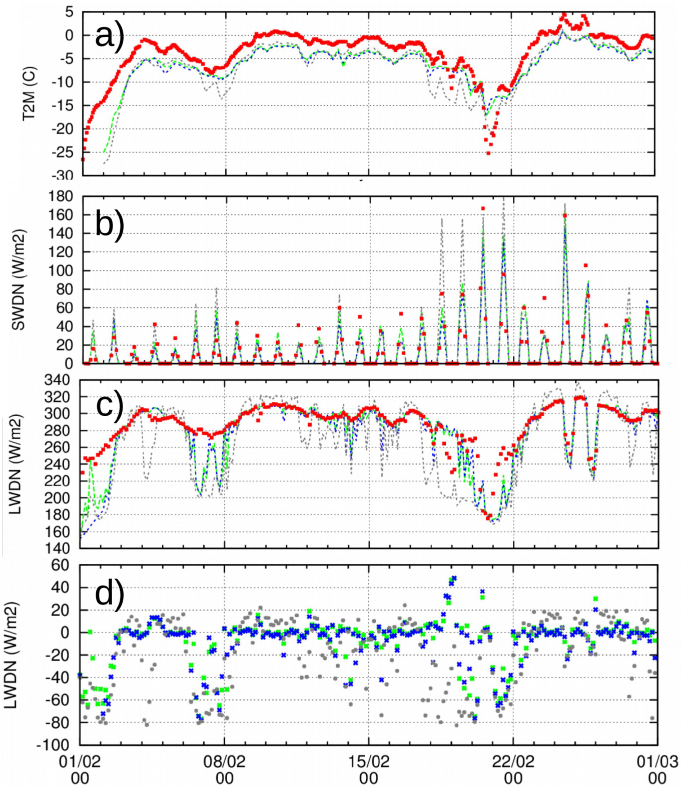

Figure 4. Variables as function of time (x axis, dates in February 2014 shown on the axis): screen-level temperature **(a)** unit: °C; SWD **(b)** and LWD **(c)**, unit $\mathrm{W\,m^{-2}}$; difference predicted – observed LWD **(d)**, unit $\mathrm{W\,m^{-2}}$. Colours of the curves and dots denote the observed (red), ACRANEB2 (green), HLRAD (grey), and IFSRAD (blue).

GID
5, 577–598, 2015